Cortex-based independent component analysis of fMRI time series.

Available online at www.sciencedirect.com

SCIENCE DIRECT®

Magnetic Resonance Imaging 22 (2004) 1493–1504

MAGNETIC RESONANCE IMAGING

Cortex-based independent component analysis of fMRI time series

Elia Formisano[a,*], Fabrizio Esposito[b], Francesco Di Salle[c], Rainer Goebel[a]

[a]*Department of Cognitive Neuroscience, Maastricht University, 6200 MD Maastricht, The Netherlands*
[b]*Institute of Neurological Sciences, Second University of Naples, 80138 Naples, Italy*
[c]*Department of Neuroradiology, University of Naples "Federico II," 80127 Naples, Italy*

Received 8 October 2004; accepted 8 October 2004

Abstract

The cerebral cortex is the main target of analysis in many functional magnetic resonance imaging (fMRI) studies. Since only about 20% of the voxels of a typical fMRI data set lie within the cortex, statistical analysis can be restricted to the subset of the voxels obtained after cortex segmentation. While such restriction does not influence conventional univariate statistical tests, it may have a substantial effect on the performance of multivariate methods.

Here, we describe a novel approach for data-driven analysis of single-subject fMRI time series that combines techniques for the segmentation and reconstruction of the cortical surface of the brain and the spatial independent component analysis (sICA) of the functional time courses (TCs). We use the mesh of the white matter/gray matter boundary, automatically reconstructed from high-spatial-resolution anatomical MR images, to limit the sICA decomposition of a coregistered functional time series to those voxels which are within a specified region with respect to the cortical sheet (cortex-based ICA, or cbICA). We illustrate our analysis method in the context of fMRI blocked and event-related experimental designs and in an fMRI experiment with perceptually ambiguous stimulation, in which an a priori specification of the stimulation protocol is not possible.

A comparison between cbICA and conventional hypothesis-driven statistical methods shows that cortical surface maps and component TCs blindly obtained with cbICA reliably reflect task-related spatiotemporal activation patterns. Furthermore, the advantages of using cbICA when the specification of a temporal model of the expected hemodynamic response is not straightforward are illustrated and discussed. A comparison between cbICA and anatomically unconstrained ICA reveals that — beside reducing computational demand — the cortex-based approach improves the fitting of the ICA model in the gray matter voxels, the separation of cortical components and the estimation of their TCs, particularly in the case of fMRI data sets with a complex spatiotemporal statistical structure.

Keywords: Functional magnetic resonance imaging; Segmentation; Cortex reconstruction; Independent component analysis; Multivariate analysis

1. Introduction

One of the major advantages of functional magnetic resonance imaging (fMRI) over the other brain mapping techniques is the potentiality to look at the relationships between brain anatomy and function noninvasively and on an individual basis. This unique feature of fMRI is fully exploited when the functional topography of the brain areas is analyzed in relation to an explicit anatomical representation of the subject's cortex. In such cases, maps of brain activation as obtained from the statistical analysis of the functional time series are visualized on a folded or morphed (inflated, flattened) computerized reconstruction of the subject's cortical surface (see, e.g., Refs. [1–6]).

In this type of approach, anatomical and functional information is merged together only at the final stage of the data analysis stream and mainly for the purpose of visualization. Recently, individual anatomical constraints have been used at an earlier stage as an additional constraint for the statistical analysis of functional imaging data [7–9]. Goebel and Singer [7] used the reconstruction of the cortical surface to restrict the detection of functional activation only to those voxels of a functional data set that lie within the cortex. This subset of voxels represents about 20% of the more than 100,000 voxel time courses (TCs) that are usually recorded. When the cortex is the target of the investigation, this subset also contains all the relevant functional

* Corresponding author. Department of Neurocognition, Faculty of Psychology, Maastricht University, 6200 MD Maastricht, The Netherlands. Tel.: +31 43 3884040; fax: +31 43 3884125.
E-mail address: e.formisano@psychology.unimaas.nl (E. Formisano).

0730-725X/$ – see front matter © 2004 Elsevier Inc. All rights reserved.
doi:10.1016/j.mri.2004.10.020

information. This simple approach has been shown to enhance the sensitivity and the specificity of conventional statistical methods by reducing the severity of the multiple-comparison problem in whole-brain fMRI experiments. Kiebel et al. [8] used more directly individual anatomical constraints in the analysis of fMRI time series by introducing the framework of anatomically informed basis functions (AIBF). AIBFs allow incorporating anatomical prior knowledge based on reconstructed gray matter surfaces into spatiotemporal models of the fMRI time series. Andrade et al. [9] showed that cortical surface-based smoothing of functional time series increases the sensitivity of conventional voxel-based approaches that rely on general linear model (GLM) parameter estimation.

In all these cases, methods employed for the functional analysis were univariate [7,9] or multivariate [8] hypothesis-driven statistical methods that require an a priori specification of a temporal model of the effects of interest. Exploratory data-driven approaches that do not make assumptions about the time profile of the effects of interest offer a complementary perspective to the conventional analysis of fMRI time series [10]. This might be especially useful in those cases in which the event of interest is not predictable (hallucinations, epileptic seizures) and when the hemodynamic response is difficult to model, such as in event-related designs with complex cognitive tasks or in experiments with perceptually ambiguous stimuli (see below).

Among data-driven methods, independent component analysis (ICA, [11]) appears to be particularly promising for the analysis of fMRI data (see Ref. [12] for a recent review). In the first applications of ICA to fMRI data analysis [13,14], the ICA variant used is *spatial* in that the observed 4D fMRI signals are modeled as linear "mixtures" of unknown spatially independent processes (e.g., BOLD signal changes related to the cognitive task, physiological pulsations, head movements, artifacts, etc.), each contributing to the data set with an unknown time profile. An adaptive ICA algorithm [15] was adopted to decompose the time series into spatial components (ICs), each having a unique TC. The decomposition process maximizes the spatial statistical independence of the components, the idea being that the new representation of the data (ICs/TCs) reflects the "unmixed" configuration of the original spatial processes. Less frequently, a temporal ICA variant has also been adopted [16–18].

In the spatial ICA (sICA), as proposed in McKeown et al. [14], the entire matrix of the fMRI time series is blindly decomposed. This matrix includes not only signals from the cerebral cortex, but also from other parts of the brain, including subcortical structures, white matter and ventricles. The resulting decomposition, thus, also models the dynamics of the signal in these other structures.

Here, we combine sICA with methods of cortex segmentation and reconstruction and restrict the sICA decomposition to the "cortical" subregion of the matrix. We use the mesh of the white matter/gray matter boundary, automatically reconstructed from T1-weighted MR images [19], to limit the spatial ICA only to those voxels of the T2*-weighted functional time series which are within a specified region with respect to the cortical sheet (cortex-based ICA, or cbICA). We expect this cortex-based approach to improve the separation and anatomical accuracy of the ICs that represent cortical cognitive activations for two reasons. First, the number of voxels included in the data matrix does not affect the maximal number of spatial components which can be obtained (it equals the number of time samples, i.e., functional scans). Exclusion of extracortical contributions to the signal data set, thus, allows using the same number of components, otherwise used to separate noninteresting processes (e.g., signal changes in the ventricles, near the eyes, imaging artifacts), only for the processes occurring on the cortical surface. Second, improvements are also expected because of consideration on how the observed spatial mixtures are influenced by the "nature" of the included signals. Signals from, for example, the ventricles or near the eyes are "uninformative" with respect to the signals on the cortex. Thus, their inclusion in the data matrix leads to an increase of the complexity of the mixtures (in terms of number of sources) but does not improve the estimation of the cortical sources. Conversely, the restricted (yet statistically acceptable) sample of spatial observations considered in the cortex-based approach is highly "informative" with respect to the "interesting" sources and may lead to a better estimation of their spatial distribution.

We illustrate the cbICA framework in the context of whole-brain fMRI block and event-related experimental designs and in an experiment with perceptually ambiguous stimuli, in which the subject's perceptual state is not known a priori. Functional MRI time series is decomposed blindly into cortical surface components (CSCs) that can be directly visualized on the folded or morphed representation of the cortex. Results are compared to the results of conventional methods of linear multiple regression and principal component analysis (PCA), as well as to anatomically unconstrained spatial ICA [14].

2. Materials and methods

2.1. General description of the cbICA approach

The steps of the cbICA are schematically illustrated in Fig. 1. Input data sets consist of a high-spatial-resolution 3D anatomical volume and a functional time series of the same subject, which have been previously coregistered (see below).

The initial steps of the cbICA approach are the generation of a *cortical mask* of each subject and the selection of a restricted functional data set consisting of the TCs corresponding to the cortical voxels in the functional time series. First, a polygonal mesh representing the white matter/gray matter border is obtained from the 3D recording of the subject (see Section 2.2). This mesh is then projected

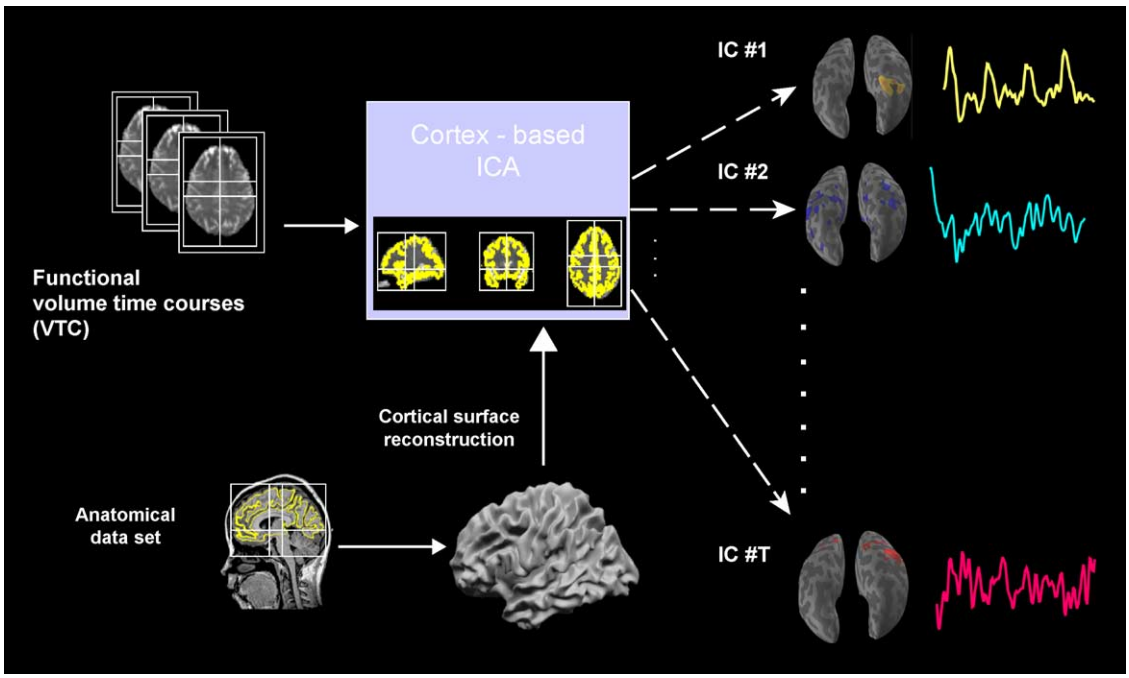

Fig. 1. Schematic representation of the cortex-based ICA approach.

into the functional volume TC (VTC) and those voxels that lie within a specified range with respect of the white matter/gray matter border are tagged as "gray matter" voxels (see Section 2.3). Finally, the data set consisting of the functional TCs is decomposed using ICA in spatially independent components, each having an associated TC (see Section 2.4). The components consist of voxel values at locations linked to the cortical surface and therefore can be directly visualized on the folded, inflated and flattened representation of the cortex (CSCs).

2.2. Generation of cortical meshes

A polygonal mesh reconstruction of both cortical hemispheres of each subject is generated from high-resolution 3D anatomical MR volumes collected during the fMRI sessions (see below). The white matter/gray matter border is segmented with a region-growing method preceded by inhomogeneity correction of signal intensity across space. The border of the resulting segmented subvolumes is tessellated to produce a polygon mesh representation of each cortical hemisphere. The tessellation of the white matter/gray matter boundary of a single hemisphere yields a polygon mesh typically consisting of approximately 250,000 triangles. Then, an iterative 3D morphing algorithm is used to move all surface vertices outward along their normals, such that the surface came to represent the spatial structure of the cortical gray matter. Through visual inspection, this process is halted when the surface reached the middle of the gray matter corresponding approximately to layer 4 of the cortex. The resulting surface is used to create the cortical mask (see below) and as spatial reference in projecting functional data onto inflated representations of the cortex.

2.3. Coregistration of functional and anatomical data and selection of cortical TCs

In order to select the functional TCs that correspond to gray matter voxels, functional slices are coregistered to the 3D anatomical volumes. Since the functional and 3D structural measurements are usually performed within the same recording session, coregistration of the respective data sets could be obtained directly based on the slice position parameters of the T2*-weighted measurement (number of slices, slice thickness, distance factor, angles, field of view, shift mean, off-center read, off-center phase, in plane resolution) and on parameters of the T1-weighted 3D T1 measurement (number of sagittal partitions, shift mean, off-center read, off-center phase, resolution) with respect to the initial overview measurement (scout). For confirmation of coregistration accuracy, a 2D anatomical data set can be obtained by reslicing the 3D data set using the slice position parameters and compared visually to the EPI data sets. Based on the parameters for importing the 2D functional slices into the 3D data sets and on the parameters for transforming the 3D data sets into Talairach space [20], the complete functional data of each subject are interpolated to 3 × 3 × 3 mm resolution (using trilinear interpolation) and transformed into Talairach space[1]. This

[1] The Talairach transformation of anatomical and functional images represents an optional step in the cbICA framework. The only critical requirement for cbICA is the precise coregistration between functional time series and anatomical volumes. Here, we have normalized our data into the Talairach space in order to take advantage of an automatic segmentation algorithm that makes use of standard masks to label subcortical structures [19].

yields a normalized 4D data representation (VTC) for each functional data set.

Since VTCs are coregistered to 3D anatomy, they are also coregistered to the polygon mesh representing the cortical sheet, which can thus be directly used to tag the cortical voxels of the functional data. The cortical mesh is projected into the functional data set and the voxels that are within a specified range were tagged as "cortex." This range is defined in millimeters along the direction of the normal vector of each vertex. A normal vector points outward, that is, into the gray matter. Its direction is orthogonal to the local surface patch surrounding a vertex. The corresponding set of functional TCs form the reduced matrix ($\mathbf{X}_c$) containing the cortical TCs which are used in cbICA.

2.4. Spatial ICA decomposition

Let $\mathbf{X}_c$ be the $T\times M_c$ (T=number of scans, M_c=number of cortical TCs) matrix of the cortical TCs (as defined in step 2), $\mathbf{C}$ the $N\times M_c$ matrix whose rows C_i ($i=1,\ldots,N$) contain the spatial processes ($N\leq T$=number of processes) and $\mathbf{A}$ the $T\times N$ mixing matrix whose columns A_j ($j=1,\ldots,N$) contain the TCs of the N processes and is assumed to be of full rank. The problem of the ICA decomposition of fMRI time series can be formulated as the estimation of both matrices of the right side of the following equation:

$$\mathbf{X}_c = \mathbf{AC} \quad (1)$$

under the constraint that the processes C_i are (in the ideal case) spatially independent. No a priori assumption is made about the mixing matrix $\mathbf{A}$, that is, about the TCs of the processes. In this model, all the spatial components, with the possible exception of one, are assumed to be non-gaussian. Structured (non-gaussian) artifacts in the data (e.g., head movements, machine and physiological artifacts) are not explicitly modeled, but instead are treated as independent sources and are thus expected to be represented in one or more of the components.

The amount of statistical dependence within a fixed number of spatial components can be quantified by means of their mutual information [11]. Thus, the ICA decomposition of $\mathbf{X}_c$ can be defined (up to a permutation of the components, a multiplicative constant and to the sign) as a linear transformation:

$$\mathbf{C} = \mathbf{WX}_c \quad (2)$$

where the matrix $\mathbf{W}$ (the "unmixing" matrix) is determined such that the mutual information of the target components C_i is minimized. Matrix $\mathbf{A}$ can be computed as the pseudo-inverse of $\mathbf{W}$.

Different ICA algorithms estimate C_i using different strategies (for a review, see Ref. [21]). Here, $\mathbf{X}_c$ was blindly decomposed with a fixed-point ICA algorithm (FastICA, [22] as implemented in http://www.cis.hut.fi/projects/ica/fastica/). The FastICA algorithm minimizes the mutual information of the components using a robust approximation of the negentropy as a contrast function and a fast, iterative (nonadaptive) algorithm for its maximization (for a detailed description of the FastICA algorithm, see Ref. [22]). After sphering the matrix $\mathbf{X}_c$ and the optional reduction of the temporal dimension of the data set with PCA (see below) the hierarchical (deflation) mode of the FastICA algorithm was used and the components were estimated one by one. Additional analysis was performed using the Infomax algorithm [15]. Results were very similar to the ones reported here. A comparison between the FastICA and the Infomax algorithms has been previously reported in [23].

2.5. Functional MRI data

We applied cbICA to fMRI data sets collected using a block design, an event-related design and in an fMRI experiment with perceptually ambiguous stimulation (see below). These data sets had been collected and analyzed using conventional statistical methods in the context of previous fMRI studies from our group [24–26].

Anatomical and functional data sets were collected at 1.5 T using a Siemens Magnetom Vision MR scanner (fMRI studies 1 and 2) or a Philips ACS-NT MR scanner (fMRI study 3), with conventional head coils and gradient echo EPI sequences (see below for acquisition parameters). Functional slices were preprocessed using 3D motion correction, slice scan time correction and high-pass filtering in the temporal-frequency domain (for details, see Refs. [24–26]). For each subject, a high-resolution anatomical data set covering the whole brain was collected during the same session as the functional measurements with a 3D, T1-weighted sequence tuned to optimize the contrast between gray vs. white matter (matrix=256×256, thickness=1 mm, number of partitions=170–180, voxel size=1×1×1 mm^3). These high-resolution 3D recordings were used for segmentation and surface reconstruction of the subjects' cortex.

2.5.1. fMRI study 1: perception of visual objects (blocked design)

Block-design data consisted of a functional time series (gradient-echo EPI, TE=60 ms, FA=90°, TR=4500 ms, FOV=200×200 mm^2, voxel size=1.6×1.6×3 mm^3, 126 scans) from a normal subject taking part in an fMRI study of blindsight patients. Colored images of natural objects (fruit and vegetables) subtending 5.2° by 5.2° were presented in the upper visual field 7° off-axis in one hemifield at a time. Each stimulation block lasted for 30 s and was repeated four times within each recording session. Stimulation blocks were separated by fixation blocks of equal length. Within a stimulation block, an image was shown for 1 s and then replaced by the next image without an interstimulus interval (for further details on experimental procedures and materials, see Ref. [24]).

2.5.2. fMRI study 2: mental imagery of clocks (event-related design)

Event-related data sets consisted of functional time series (gradient-echo EPI, TE=60 ms, FA=90°, TR=2000 ms, FOV=180×180 voxel size=2.8×2.8×5 mm^3, 16 slices, 126 scans per time series) from two normal subjects participating in an fMRI study of visuospatial mental imagery. Subjects were asked to imagine two analog clock faces corresponding to 2 h verbally presented (e.g., 9:30 and 10:00) and to push a button with her index finger if the hands of the first clock formed the greater angle or with their middle finger if the hands of the second clock formed the greater angle. The intertrial interval was 16 s. In each trial a different pair of hours was presented. Each subject performed four functional runs. The hand used for the button press response was counterbalanced across runs in an A-B-B-A design (for further details on experimental procedures and materials, see Ref. [25]).

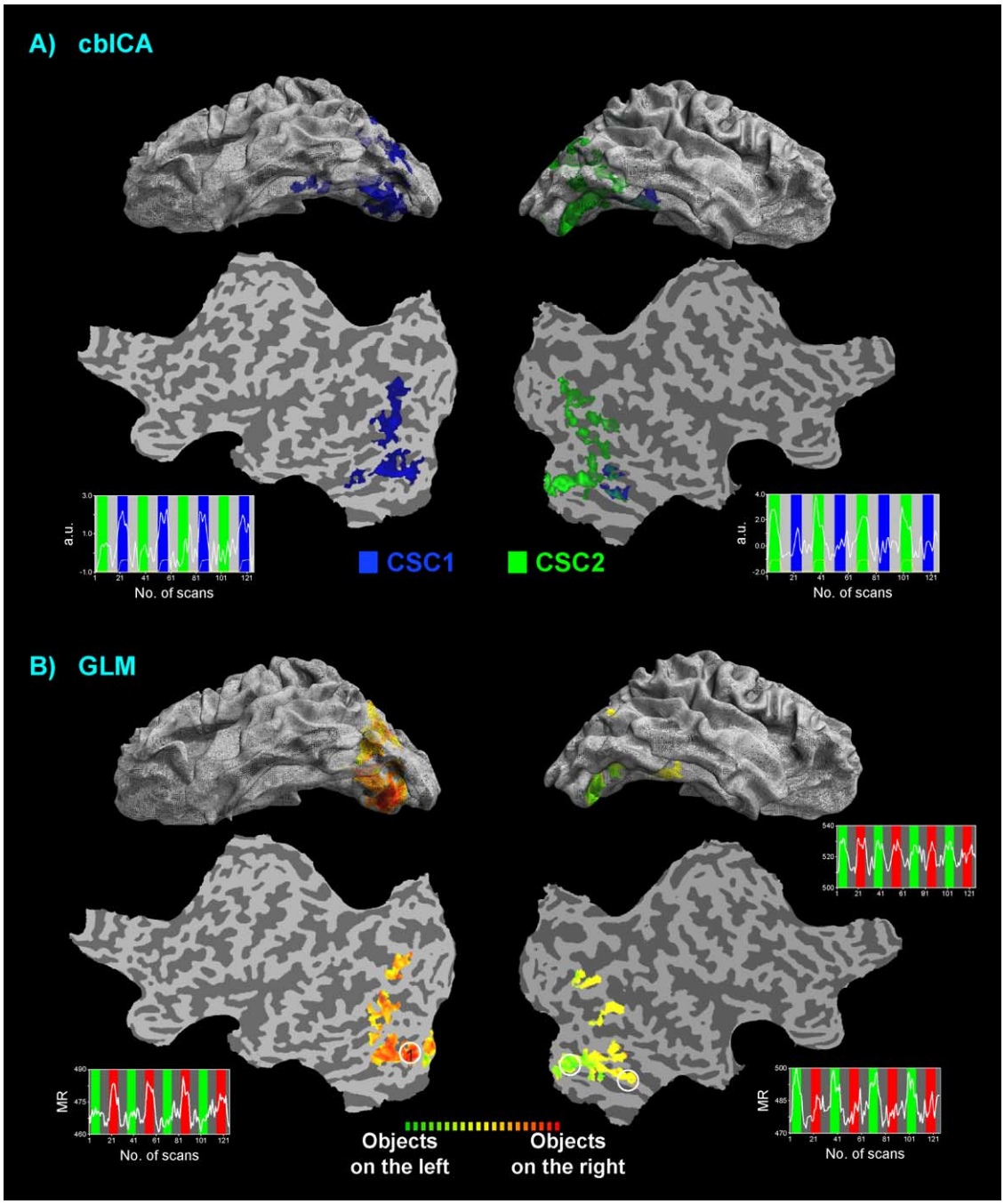

Fig. 2. Results of a cbICA decomposition and a GLM analysis for a functional data set collected using a block-designed protocol with two alternating conditions of visual stimulation (see text). Two cortical components with highly task-related TCs (R=.76, .73) were obtained, which identified correctly the same areas identified by the GLM (P<.001, corrected).

2.5.3. fMRI study 3: ambiguous perception of moving plaids

Functional time series (gradient-echo EPI, TE=40 ms, TR=2083 ms; FA=90°, FOV=224×224 mm^2, 22 slices, voxel size: 3.5×3.5×5 mm^3) from two subjects participating in an fMRI study on motion perception were analyzed using cbICA. Stimuli were two moving gratings (surfaces) superimposed in the same display (plaids). Depending on specific parameters of the stimuli (contrast, luminance of the intersection), these surfaces can either be perceptually segregated and perceived as one grating sliding on top of the other (component motion) or perceptually integrated into a single surface that moves in a direction intermediate to the motion directions of the component gratings (pattern motion). Certain configurations of plaid stimuli can lead to bi-stable interpretations with spontaneous switches between perceptual integration (pattern motion) and segregation (component motion). This experiment took advantage of these "ambiguous" plaids stimuli to investigate whether activity patterns in human motion-sensitive areas depend on the interpretation of global motion. Periods of stimulation with bi-stable moving plaids were alternated with periods during which stationary plaids were presented (~16-s period). During the motion periods, subjects were required to report with a button press the perceptual interpretation of the stimulus (component or pattern). It is important to remark that in this experiment the stimulation protocol is not under control of the experimenter because during the motion condition the stimulus is physically constant and the conditions of interest (component motion and pattern motion) are only defined by internal percept changes (for further details on experimental procedures and material, see Ref. [26]).

2.6. Selection of the components of interest and comparison of cbICA with conventional spatial ICA

We compared the results of the cbICA approach with those of conventional, anatomically unconstrained, spatial ICA (referred to as volume-based ICA, or vbICA) on the basis of (1) the analysis of spatial maps and TCs of components of interests that reflected stimulus-related processes; and (2) a quantitative analysis of the global statistical properties of the ICA decompositions as reflected by the −log-likelihood function [23,27].

2.6.1. Analysis of components of interest

In the first analysis, components of interest were selected as follows. In study 1 (block design) and study 2 (event-related design) we selected from the set of surface maps obtained for each data set a subset of components defined by the conjunction of two criteria: (1) the IC TC was significantly correlated ($P<.001$) with the model employed in the conventional GLM analysis; (2) the IC spatial map presented at least one 3D cluster of voxels with size >300 mm^3, all with $|Z|$ normalized values >2. Additionally, in study 2, we temporally sorted the selected components according to the onset time of the associated TC. The onset

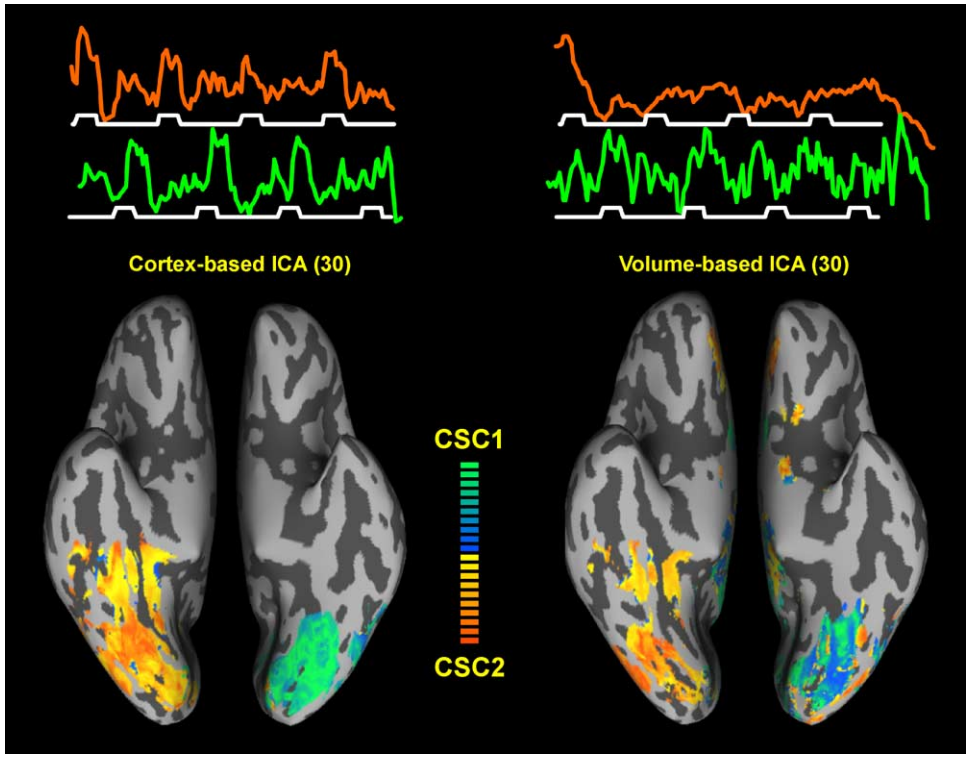

Fig. 3. Comparison between cbICA and anatomically unconstrained sICA (vbICA) decomposition using the same number of components (=30) and the same z threshold ($z>2$). The spatial layout and the TCs of the pair of cortical components obtained with the cbICA were considerably more accurate than the ones obtained with the vbICA.

time was defined as the time (measured from the stimulus onset) at which the TC reached 10% of its peak value. In study 3, the components of interest were selected exclusively on the basis of a spatial criterion (see Section 3.3).

2.6.2. Log-likelihood analysis

We compared the global statistical properties of the ICA decompositions obtained with our approach and with the conventional approach to a likelihood analysis [27]. This analysis provides an estimate of how significantly a fixed number of ICs can theoretically predict new observations in the same conditions, assuming that the basic ICA model in Eq. (1) actually holds.

The procedure stems from the property of the ICA model to be a generative model (i.e., there is no error term or any kind of residuals) and allows the posterior estimate of the "goodness-to-fit" of a decomposition. Formally, we estimated the unmixing matrix **W** of Eq. (2) by using each of the two ICA approaches and then we estimated the probability of observing the jth voxel TC under the model specified in Eq. (1), as described in Ref. [27]. A global figure of merit was obtained for each data set by averaging across voxels the log-likelihood estimates obtained at each voxel. This parameter can be computed for an ICA decomposition for a varying number of target components, provided that, for $N<T$, the remaining $T-N$ rows of **W** are filled using a partial PCA decomposition previously removed in a dimension-reduction preprocessing step. The case $N=0$ (i.e., no ICA performed) corresponds to a simple PCA decomposition. Higher values for this figure indicate a lower goodness-to-fit and so a worse model estimation and vice versa. In Ref. [27], this same likelihood analysis was used to make inferences about the optimal number of principal components to be selected by means of a preliminary PCA. Here, it is used only with the purpose of a relative comparison between the cbICA approach and the conventional, anatomically unconstrained sICA (see Fig. 4).

3. Results

3.1. Experiment 1 (blocked design)

Fig. 2A shows the components (referred to as CSC1 and CSC2) corresponding to the cortical response to the visual stimulation (objects presented in the right and left visual hemifield alternately). CSC1 and CSC2 are the two components whose TCs were most highly correlated ($R=.76$ and $R=.73$) with hemodynamic predictor functions computed on the basis of the stimulation protocol by a linear model. The component maps were projected onto the folded and flattened representation of the subject's cortex. The brain areas integrated in these components included all early visual areas in the occipital cortex and in the ventral stream that responded to the presentation of the objects in the contralateral hemifield. Early areas of the visual processing stream were represented in a single component, while more ventral areas received the contribution of both the components (see Fig. 2A, blue patch in right hemisphere), indicating that their response was less selective to the hemifield of stimulation. The spatial locations of these areas corresponded very well to the locations of the areas identified by the multiple regression analysis (see Fig. 2B).

Fig. 3 shows the comparison between cbICA and vbICA at a fixed number of components (number of components=30). In both cases, the two components that mostly correlated to the stimulation protocol were selected. A visual inspection of the CSCs shows that the cortex-based decomposition lead to a more accurate estimate of the spatial layout and of the TCs of the task-related cortical activations than a conventional sICA decomposition using the same number of components. In particular, the estimate of the TC of CSCs was drastically improved by the cortex-based approach.

These qualitative differences between cortex-based and conventional ICA were also reflected in a quantitative evaluation performed with a log-likelihood analysis. For a varying number of components, an estimate of the $E\{-\log\text{-likelihood}\}$ was obtained for both conventional and cortex-based ICA by averaging the voxelwise values (1) across all voxels included in the ICA decomposition and (2) across the common subset of gray matter voxels (Fig. 4A). When

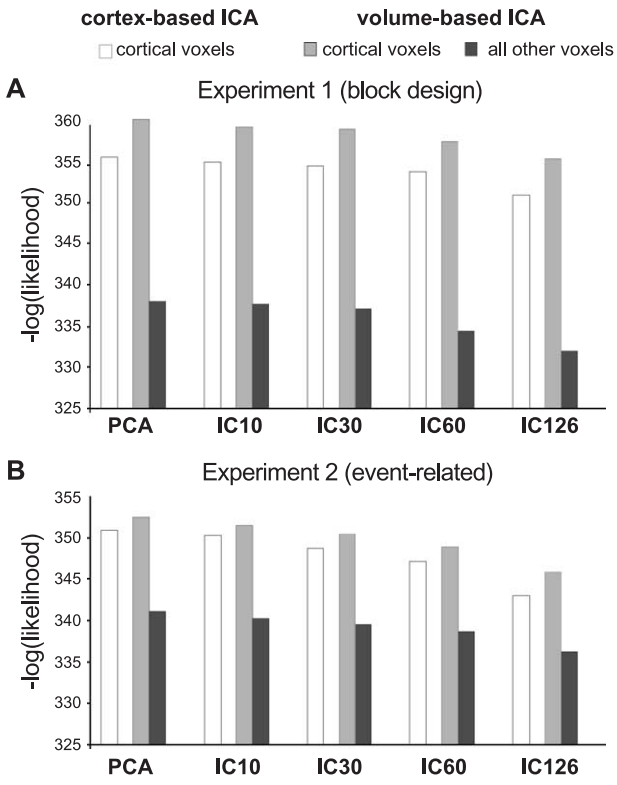

Fig. 4. Analysis of the −log-likelihood function for the cbICA and the vbICA for Experiments 1 (block design, A) and 2 (event-related, B). Lower values of this function indicate a better fit of the ICA model. The vbICA model fits better in the extracortical than cortical voxels. The cbICA model fits better than the vbICA model in the cortical voxels.

computing the mean of the −log-likelihood function across all voxels, lower values (indicating a better fit to the data) were obtained for the vbICA. This apparent contradiction with the qualitative analysis of the CSCs is easily explained by considering that many of the voxels included in the vbICA are white matter voxels. In these voxels, the signal is simpler and much lower values of −log-likelihood are expected [27]. Indeed, when $E\{-\text{log-likelihood}\}$ was computed for both approaches on the same subset of gray matter voxels, lower values were obtained in the case of the cbICA. This confirms the results of the qualitative analysis and indicates that, when using the same number of components, cbICA is better suited than vbICA for the modeling of fMRI signals from gray matter voxels.

3.2. Experiment 2 (event-related design)

Fig. 5 illustrates the results of the ICA decomposition of individual fMRI time series in the case of the event-related fMRI experiment. The subsets of cortical components whose TCs reflected task-related activation were selected and projected on the flattened representation of the subject's cortex. In the case of complete ICA decomposition ($N=T=126$, Fig. 5, middle panel), surface maps and TCs of task-related components accurately

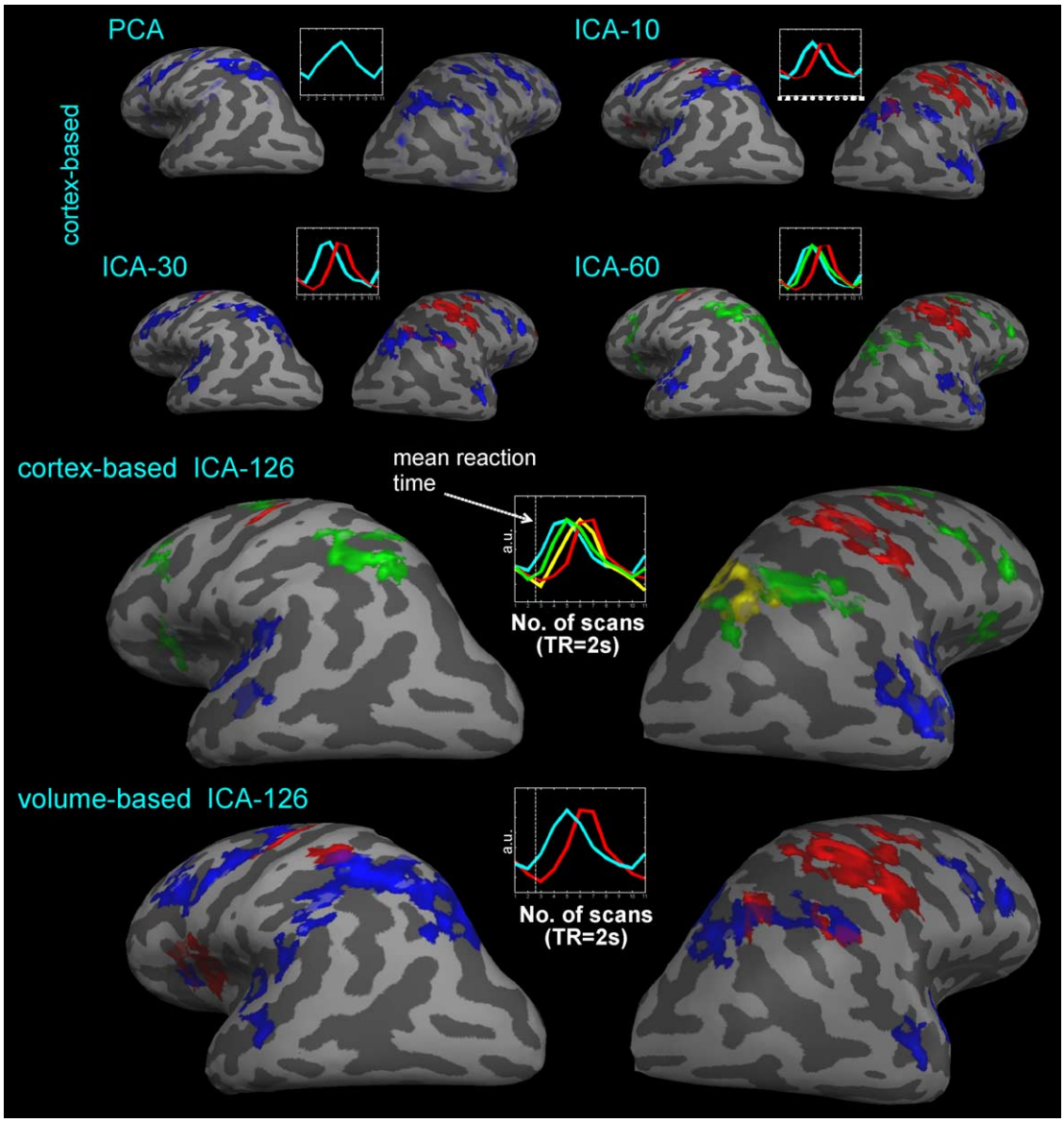

Fig. 5. Cortex-based PCA, cortex-based ICA (with IC = 10, 30, 60 and 126) and volume-based ICA (IC = 126) of an event-related functional data set from a study of visuospatial imagery [25]. Each task-related CSC and the corresponding event-averaged TCs are indicated with a different color. By increasing the dimensionality of the decomposition, the cbICA identified with increasing accuracy the spatial layout of the cortical areas involved in the successive processing stages required by the task (auditory cortex, frontoparietal areas and sensorimotor cortex; see text) and their TCs of activation. The volume-based ICA yielded results comparable, in terms of spatial layout and estimated TCs, to the cbICA-30 but considerably poorer than the cortex-based ICA with the same number of components.

confirmed the topography as well as the sequence of activation of the brain regions that were obtained with the hypothesis-driven analysis (for a comparison, see Ref. [25]). Indeed, the subset of task-related components included separate components that reflected the sequential activation of the transverse temporal gyrus and of the superior temporal sulcus bilaterally (blue), of frontoparietal regions (green and yellow) and of the sensorimotor cortex contralateral and, at minor extent, ipsilateral to the response hand (red). The components corresponding to the frontoparietal activation showed very typical spatiotemporal features. The first component (green) had clusters located mainly, but not exclusively, in the left posterior parietal cortex (PPC). Additional clusters were also present in the right PPC and, in some cases, in the dorsolateral prefrontal cortex. The second component (yellow) was highly lateralized with clusters almost exclusively located in the right PPC on the superior part of the intraparietal sulcus. The TCs of these two components were consistent with the results of the conventional analysis, and the activation of the component lateralized in the right PPC followed the activation of the other, less lateralized, component.

The upper panel of Fig. 5 shows the results of using cortex-based PCA, and ICA after a PCA-based dimensionality reduction to 10, 30 and 80 components. It is evident that, for this event-related fMRI data set, a reduction of dimensionality had a negative effect on the differentiation of the spatiotemporal pattern of cortical activation. These results suggest that caution should be taken in reducing

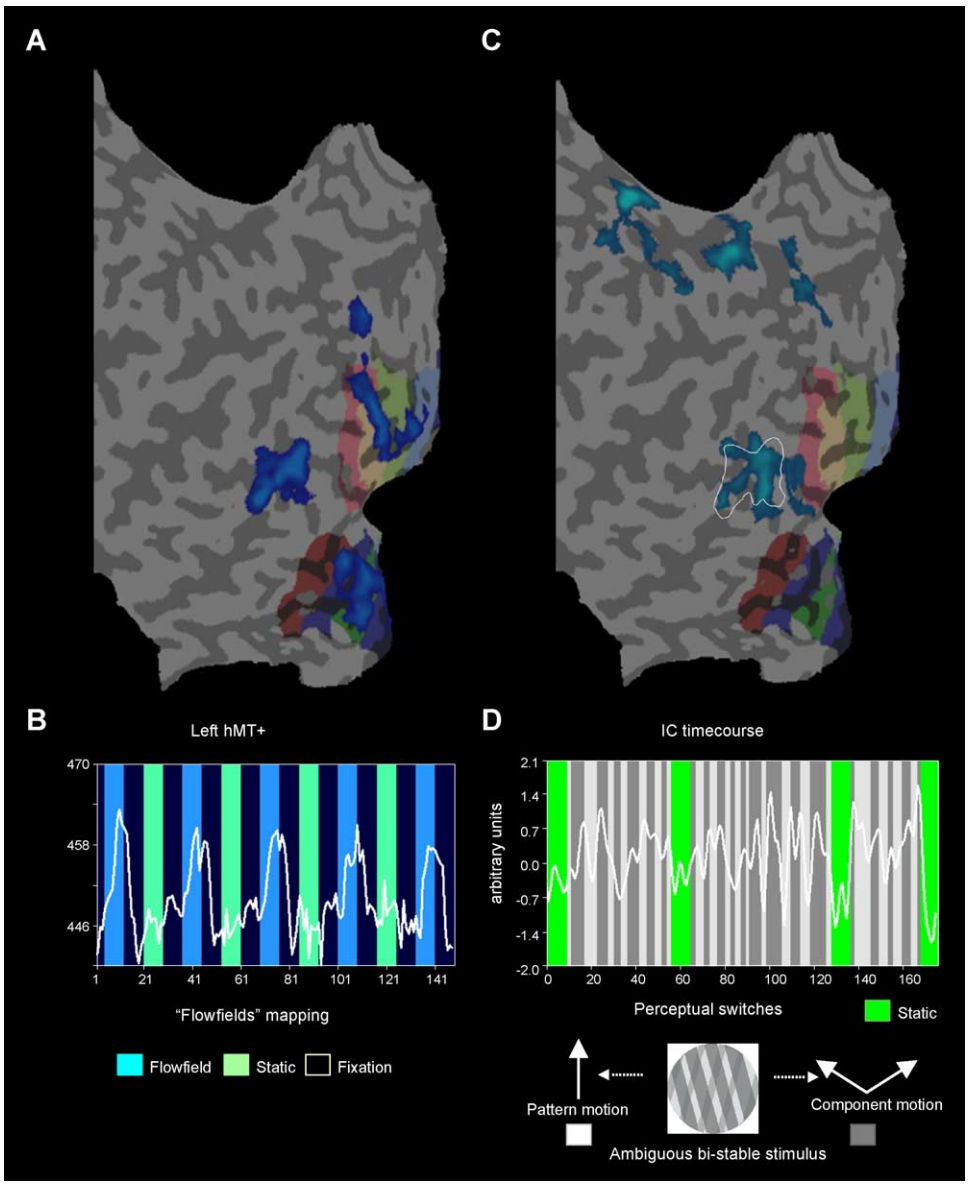

Fig. 6. Application of cbICA to an experiment with ambiguous stimuli. A region of interest (hMT+/V5) was defined in each subject by means of a mapping experiment and conventional analysis (A, B). This region was then used for an automated selection of interesting independent components. The spatial layout (C) and the TC (D) of the selected component reveal the involvement of hMT+/V5 during the perceptual switches.

excessively the dimensionality of fMRI time series previous to their ICA decomposition (see Section 4).

The lower panel of Fig. 5 shows the results of a conventional anatomically unconstrained ICA decomposition (with no dimensionality reduction) of the same data set. Compared to the cbICA, this analysis gave much poorer results and only two task-related components were detected. Note that these results are comparable to the cbICA decomposition with a dimensionality reduction with $N=30$ (Fig. 5, upper panel).

Fig. 4B shows the results of the log-likelihood analysis that, as in the case of the block design, was performed in these event-related data sets to compare the cbICA with the vbICA. Again, lower values of $E\{-\text{log-likelihood}\}$ were obtained for the cortex-based approach when the averaging was limited to the gray matter voxels, indicating that in these locations the cbICA model fits better than the vbICA model.

3.3. Experiment 3 (ambiguous plaids)

Fig. 6 highlights the value of ICA as a method to analyze data with irregular and unpredictable perceptual periods, as it is the case for ambiguous plaids stimuli. During the stimulation with ambiguous plaids stimuli, subjects reported (using a button press) frequent percept changes between component and pattern motion (see different background colors in the TC panel). Based on previous data [26], it was expected that these changes would be reflected in the activity of the motion complex hMT+. This possibility was investigated using cbICA. First, a region of interest (hMT+/V5) was defined for each subject on the basis of a conventional statistical analysis of a functional mapping experiment (flow-field mapping, Fig. 6A and B). Successively, the component presenting the highest peak values in hMT+/V5 in the experiment with ambiguous stimuli was selected automatically and independently of its TC. This latter was analyzed post hoc with reference to the subject's report. Note that this approach does not rely on any a priori specification of the temporal profile of the hemodynamic response and removes potential interpretation biases caused, for example, by the choice of a specific hemodynamic delay. Fig. 6C and D shows the selected CSC, the corresponding TC and its relation with the subject's report. Importantly, this CSC includes not only hMT+/V5 but also sensorimotor-related regions, activated because of the button press. This result suggests that, during the perception of the moving plaids, hMT+/V5 was part of a functionally connected network of regions involved in the perceptual decision.

4. Discussion

Cortex-based ICA is an approach for the analysis of fMRI data that combines techniques for the reconstruction and morphing (inflation, flattening) of the cortex from anatomical MR images with sICA of functional time series. We have demonstrated the validity of this approach by analyzing various fMRI data sets collected with different experimental designs (blocked and event-related designs, ambiguous stimulation) and by comparing the results we obtained with those of conventional hypothesis-driven statistical methods and with anatomically unconstrained sICA.

The comparison between cbICA and conventional univariate statistical methods showed that cbICA could replicate "blindly" the results of the multiple regression analysis and detect spatial patterns and TCs of task-related cortical activations, both in a blocked and in an event-related design. This is not surprising because the sICA is a linear transformation of the data and the overall pattern of activation contained in the subset of task-related components has to be very similar to the activation pattern obtained with a multiple linear regression analysis if an appropriate design matrix is used. Yet the representation of the time series in the signal subspace defined by the sICA transformation can be very informative and might reveal interesting properties of the data that would remain hidden with the hypothesis-led analysis alone. This point is clearly illustrated by the results of the cbICA decomposition of our event-related data. The sequence of brain activation detected with this data-driven analysis is consistent with the conventional analysis in [25]. However, compared to the univariate statistical maps, the cbICA representation clearly highlights the contribution of distinct networks of areas to different stages of the task. Spatially remote brain regions that most probably are simultaneously involved in the same stage of the task are indeed included in the same component [see, e.g., bilateral auditory and language regions (blue) for the early stages and bilateral sensorimotor regions for the late stages (red)]. Also, the frontoparietal activation is separated into two components, one more distributed and bilateral (green) and the other localized in the right PPC (yellow). This separation is likely to reflect the involvement of the bilateral network and the right PPC in the early and late stages of the task, respectively (presumably, generation and spatial analysis of mental images, see Ref. [25]).

The "functional" meaningfulness of the observed separation/grouping of brain regions in the various components is supported by several additional analyses and considerations that allowed to safely exclude that this was not caused by methodological factors, such as, for example, the artifactual fractioning of a single component (see below). First, a trial-by-trial estimation of onset latency, width and amplitude of the hemodynamic responses in all areas confirmed their actual differences. Second, different patterns of correlations between trial-by-trial reaction times and estimated HR parameters were found, confirming the hypothesis of the involvement of the various brain regions in different stages of the task [25]. Finally, in a subsequent study using repetitive transcranial magnetic stimulation and the same task, significantly slower RTs were observed when the right, but not the left, PPC was transiently suppressed by an rTMS coil [28], thus bringing additional support to the view of differential function roles of the parietal components [29].

Both a qualitative and a quantitative comparison between cbICA and anatomically unconstrained sICA revealed the advantage of using a cortex-based approach to estimate cortical processes as spatially independent components. Compared to the conventional approach and using the same number of components, cbICA lead to a more accurate estimation of spatial layout and TCs of task-related activations in block-designed as well as in event-related experiments. Similarly, the global comparison between the two methods performed using the log-likelihood analysis indicates a better performance of cbICA. Crucial to the application of the cbICA approach is the availability of an accurate reconstruction of each individual cortex and of an accurate coregistration between functional and anatomical data. In practice, this ensures an adequate selection of gray matter voxels. Due to partial volume effects and to the different resolution of functional and anatomical images, however, uncertainty can arise for the functional voxels at the border of the cortex. To avoid the exclusion of any cortical contribution, we used a conservative approach and considered as gray matter all the voxels at the cortical border. In the future, the improved spatial resolution of functional images [5] together with methods for the tagging of the voxels based on the explicit modeling of inner and outer cortex boundary will allow increasing the selectivity of this labeling. Alternatively, voxels may be treated using a probabilistic approach in which a voxel's contribution to the data set is weighted according to its likelihood to be gray matter [30]. However, because voxels at the gray matter/white matter border only represent a small proportion of the data, no great differences in the results are expected.

The results of the analyses presented in this paper suggest additional considerations on important issues of ICA-fMRI methodological research. The first regards the choice of the number of components/dimensions to be considered in the ICA decomposition. Dimensionality reduction via simple PCA is a conventional preprocessing step in the ICA of fMRI time series and has useful filtering and computational properties. This step requires choosing the number of components for the ICA decomposition. Setting this number too high may result in functionally connected regions split into separate components (overfitting). An excessive reduction of the dimensionality, on the other side, may be particularly problematic for the analysis of complex fMRI data sets because the interesting sources are expected to be "weak" compared to other, artifactual sources. Generally, the dimensionality of the signal space (i.e., the selection of the number of components) is chosen by selecting the eigenmodes associated with the highest eigenvalues after analyzing the eigenspectrum either by visual inspection or by means of more objective criteria [30]. Our analysis of the mental chronometry data shows that the spatiotemporal patterns of task-related activation were estimated better when the PCA preprocessing step was not performed at all (i.e., with the maximum number of available components). This implies that relevant information for detecting fine-grained differences between activation patterns was contained in the "low" part of the eigenspectrum and that the effects of reducing the dimensions to the highest eigenvalues should be, at least, cautiously examined.

A second point regards the treatment of spatially varying latencies of the hemodynamic responses. A recent approach proposes to completely remove the latency information and perform the ICA on the amplitude of the spectrum of FFT-transformed TCs (see Ref. [31]). In this way, brain regions that differ only in latency are grouped in the same component; the latency is then estimated post hoc voxel by voxel. Conversely, the original approach [14] and our ICA approach assume that the TCs of cortical areas within one component are synchronous and thus results in the representation of areas with TCs that differ in latency in separate components. In principle, both the approaches are useful to analyze event-related fMRI data sets. However, in fMRI mental chronometry studies such as the one described in this paper, latency differences as well as differences in other aspects of the response (e.g., width) are meaningful and experimentally induced. For this type of studies, thus, a representation with separate components seems to be the most appropriate in that it highlights the differences among the networks of areas.

The analysis of the experiment with ambiguous stimuli illustrates the advantage of using ICA-based methods when the experimenter is not under control of the stimulation protocol and the analysis based on a temporal a priori model of the response is problematic. In this case, we selected the component of interest based on a strong a priori expectation about the localization of the effect (hMT+) (see Ref. [32] for a similar approach) and examined post hoc the relation of the TC of the selected component with the behavioral measurement (button press). New methods for the post hoc selection of the interesting components that do not rely on strongly constraining spatial or temporal hypotheses promise to facilitate the use of ICA in the investigation of unpredictable or transient neural events also when a strong spatial hypothesis is not possible [33,34].

Finally, it is worth remarking that although the method presented in this paper can be used exclusively for the analysis of single-subject data sets, it can be extended to the analysis of group data by combining methods for the cortical realignment of subjects and algorithms for multi-subject ICA [35,36].

References

[1] Sereno MI, Dale AM, Reppas JB, Kwong KK, Belliveau JW, Brady TJ, et al. Borders of multiple visual areas in humans revealed by functional magnetic resonance imaging. Science 1995;268:889–93.

[2] Goebel R, Khorram-Sefat D, Muckli L, Hacker H, Singer W. The constructive nature of vision: direct evidence from functional magnetic resonance imaging studies of apparent motion and motion imagery. Eur J Neurosci 1998;10:1563–73.

[3] Dale AM, Fischl B, Sereno MI. Cortical surface-based analysis. I. Segmentation and surface reconstruction. Neuroimage 1999;9:179–94.

[4] Van Essen DC, Lewis JW, Drury HA, Hadjikhani N, Tootell RB, Bakircioglu M, et al. Mapping visual cortex in monkeys and humans using surface-based atlases. Vision Res 2001;41:1359–78.
[5] Formisano E, Kim DS, Di Salle F, van de Moortele PF, Ugurbil K, Goebel R. Mirror-symmetric tonotopic maps in human primary auditory cortex. Neuron 2003;40:859–69.
[6] Wandell BA, Chial S, Backus BT. Visualization and measurement of the cortical surface. J Cogn Neurosci 2000;12:739–52.
[7] Goebel R, Singer W. Cortical surface-based statistical analysis of functional magnetic resonance imaging data. Neuroimage 1999;9:S64.
[8] Kiebel SJ, Goebel R, Friston KJ. Anatomically informed basis functions. Neuroimage 2000;11:656–67.
[9] Andrade A, Kherif F, Mangin JF, Worsley KJ, Paradis AL, Simon O, et al. Detection of fMRI activation using cortical surface mapping. Hum Brain Mapp 2001;12:79–93.
[10] Lange N, Strother SC, Anderson JR, Nielsen FA, Holmes AP, Kolenda T, et al. Plurality and resemblance in fMRI data analysis. Neuroimage 1999;10:282–303.
[11] Comon P. Independent component analysis, a new concept? Signal Process 1994;36:287–314.
[12] McKeown MJ, Hansen LK, Sejnowsk TJ. Independent component analysis of functional MRI: what is signal and what is noise? Curr Opin Neurobiol 2003;13:620–9.
[13] McKeown MJ, Jung TP, Makeig S, Brown G, Kindermann SS, Lee TW, et al. Spatially independent activity patterns in functional MRI data during the stroop color-naming task. Proc Natl Acad Sci U S A 1998;95:803–10.
[14] McKeown MJ, Makeig S, Brown GG, Jung TP, Kindermann SS, Bell AJ, et al. Analysis of fMRI data by blind separation into independent spatial components. Hum Brain Mapp 1998;6:160–88.
[15] Bell AJ, Sejnowski TJ. An information-maximization approach to blind separation and blind deconvolution. Neural Comput 1995;7: 1129–59.
[16] Biswal BB, Ulmer JL. Blind source separation of multiple signal sources of fMRI data sets using independent component analysis. J Comput Assist Tomogr 1999;23:265–71.
[17] Calhoun VD, Adali T, Pearlson GD, Pekar JJ. Spatial and temporal independent component analysis of functional MRI data containing a pair of task-related waveforms. Hum Brain Mapp 2001;13:43–53.
[18] Seifritz E, Esposito F, Hennel F, Mustovic H, Neuhoff JG, Bilecen D, et al. Spatiotemporal pattern of neural processing in the human auditory cortex. Science 2002;297:1706–8.
[19] Kriegeskorte N, Goebel R. An efficient algorithm for topologically correct segmentation of the cortical sheet in anatomical MR volumes. Neuroimage 2001;14:329–46.
[20] Talairach J, Tournoux P. A coplanar stereotactic atlas of the human brain. Stuttgart: Thieme Verlag; 1988.
[21] Hyvärinen A, Oja E. Independent component analysis: algorithms and applications. IEEE Trans Neural Netw 2000;13:411–30.
[22] Hyvärinen A. Fast and robust fixed-point algorithms for independent component analysis. IEEE Trans Neural Netw 1999;10:626–34.
[23] Esposito F, Formisano E, Seifritz E, Goebel R, Morrone R, Tedeschi G, et al. Spatial independent component analysis of functional MRI time-series: to what extent do results depend on the algorithm used? Hum Brain Mapp 2002;16:146–57.
[24] Goebel R, Muckli L, Zanella FE, Singer W, Stoerig P. Sustained extrastriate cortical activation without visual awareness revealed by fMRI studies of hemianopic patients. Vision Res 2001;41:1459–74.
[25] Formisano E, Linden DE, Di Salle F, Trojano L, Esposito F, Sack AT, et al. Tracking the mind's image in the brain I: time-resolved fMRI during visuospatial mental imagery. Neuron 2002;35:185–94.
[26] Castelo-Branco M, Formisano E, Backes W, Zanella F, Neuenschwander S, Singer W, et al. Activity patterns in human motion-sensitive areas depend on the interpretation of global motion. Proc Natl Acad Sci U S A 2002;99:13914–9.
[27] McKeown MJ, Sejnowski TJ. Independent component analysis of fMRI data: examining the assumptions. Hum Brain Mapp 1998;6:368–72.
[28] Sack AT, Sperling JM, Prvulovic D, Formisano E, Goebel R, Di Salle F, et al. Tracking the mind's image in the brain II: transcranial magnetic stimulation reveals parietal asymmetry in visuospatial imagery. Neuron 2002;35:195–204.
[29] Formisano E, Goebel R. Tracking cognitive processes with functional MRI mental chronometry. Curr Opin Neurobiol 2003;13:174–81.
[30] Beckmann CF, Smith SM. Probabilistic independent component analysis for functional magnetic resonance imaging. IEEE Trans Med Imaging 2004;23:137–52.
[31] Calhoun VD, Adali T, Pekar JJ, Pearlson GD. Latency (in)sensitive ICA. Group independent component analysis of fMRI data in the temporal frequency domain. Neuroimage 2003;20:1661–9.
[32] van de Ven VG, Formisano E, Prvulovic D, Roeder CH, Linden DE. Functional connectivity as revealed by spatial independent component analysis of fMRI measurements during rest. Hum Brain Mapp 2004;22:165–78.
[33] Formisano E, Esposito F, Kriegeskorte N, Tedeschi G, Di Salle F, Goebel R. Spatial independent component analysis of functional magnetic resonance imaging time-series: characterization of the cortical components. Neurocomputing 2002;49:241–54.
[34] Formisano E, De Martino F, Gentile F, Balsi M, Esposito F, Di Salle F, et al. Classification of fMRI-independent components in a multidimensional feature space using least-square support vector machines. Hum Brain Mapp Abstract 2004 [Budapest, Hungary].
[35] Calhoun VD, Adali T, Pearlson GD, Pekar JJ. A method for making group inferences from functional MRI data using independent component analysis. Hum Brain Mapp 2001;14:140–51.
[36] Formisano E, Calhoun VD, van Atteveldt N, Esposito F, Di Salle F, Pekar JJ, et al. Analysis of group fMRI data with cortex-based intersubject alignment and independent component analysis. Hum Brain Mapp Abstract 2003 [New York].